



Optical Properties of Lithium Niobate Nanoparticles Prepared by Laser Ablation in Different Surfactant Solutions

¹Marwa S. Alwazny*, ²Raid A. Ismail, ²Evan T. Salim

¹Department of Laser and Optoelectronics Engineering, University of Technology – Iraq

²Department of Applied Sciences, University of Technology – Iraq

Article information

Article history:

Received: March, 16, 2022

Accepted: August, 23, 2022

Available online: March, 10, 2023

Keywords:

Energy gap,
Extinction coefficient,
Lithium-niobate,
Z-cut wafer

*Corresponding Author:

Marwa S. Alwazny

marwa.s.mohsin@uotechnology.edu.iq

Abstract

In this paper, the optical, structural, and surface morphology of novel lithium-niobate (LN) colloidal synthesis by ablation in liquid using a pulse laser method has been studied and analyzed for the first time. LiNbO₃ suspensions are synthesized using a Q-switch Nd-YAG laser with two target types, each with three different types of liquid environments: deionized water, ethanol, and acetone. The prepared colloidal is to go under further processes to be later used in the photonic application. The optical properties of the suspensions were evaluated by ultraviolet-visible (UV-Visible) measurements. The results showed that the colloidal had a transmission spectrum ranging between 88 to 98% for LN Target and 96 % to 98% for LN Z-cut wafer. The estimated energy gaps are (3.3-3.7 eV) for the prepared target and (4.1-4.3) for the LN Z-cut wafer, which gives good accordance with reported results in the range of ~ 3.7- 4 eV for all samples. In general, the Z-cut wafer target gives better results with ethanol based on optical properties. XRD measurements show the formation of a multi-phase with impurities for a prepared lithium niobate target and multi-phase LiNbO₃ films with no impurities or a second phase for another Z-cut wafer. FESEM scan is measured for LiNbO₃ films, and the particle size is about 20 and 23 nm.

DOI: [10.53293/jasn.2022.4663.1151](https://doi.org/10.53293/jasn.2022.4663.1151), Department of Applied Sciences, University of Technology

This is an open access article under the CC BY 4.0 License.

1. Introduction

Lithium niobate (LiNbO₃) is indeed a very remarkable human-made dielectric material that does not occur in nature found to be ferroelectric in 1949 [1],[2]. In recent years nano size LN has gained an increasing concern due to the remarkable combination of its physical properties for instant piezoelectric, photoelectric, acoustic-or/and electro-optical along with non-linear properties [3]. From a material perspective, the structuring of lithium niobate is very critical since it has particular properties, especially its optical one which differs from those of semi-conductors materials [4]. These outstanding characteristics are the electro-optical besides acousto-optical properties that have the strongest influence on any optoelectronics device manufacturing process. Due to these extraordinary effects of Lithium niobate display, a wide range of applications can be introduced, such as waveguide, sensor, modulator, laser surface acoustic wave (SAW) devices[5], optoelectronics devices even biosensor[6], [7], and waveguide devices [8]. LiNbO₃ were prepared using many techniques such as spray

pyrolysis [9], spin coating [10], metal-organic chemical vapor deposition (MOCVD) [11], ION PLATING method [12], and pulsed laser deposition (PLD) [13], [15]. J. Gonzalo et. al. [16] used the pulsed laser deposition technique in a vacuum using a different buffer gas environment and investigated LN films characteristics, many other researchers used this technique effectively and investigated the effect of oxygen pressure on the nanocrystalline structure of the growing LiNbO_3 [17]. Yet to our knowledge, no researcher used laser ablation in different liquid environment methods (PLAL) to prepare LN. Ablation by laser for a solid pellet in liquefied phase surrounding is adequate an extremely common strategy to control nanoparticle synthesis. This method considers a chemically straightforward, efficient and spotless synthesis process due to a decrease in by-product fabrication, Modest starting materials without the requirement for a catalyst [18]. It also demands atmospheric requirements with no radical need for high temperature or extreme pressure. Size control has been demonstrated to be possible, using PLAL by adjusting the laser wavelength, number of pulses, fluency, and liquid environment. [19], [20], [21]. First, the liquid environment in a laser ablation system can control the plasma pressure onto the target surface; the pressure is directly proportional to the density of the ablation liquid. Therefore, it may vary the size, structure, and morphology of the obtained nanostructure materials. Furthermore, the accumulation of the final product can be influenced by the liquid environment nature like dispersion or polarity [22]. For the first time, an attempted to prepare LiNbO_3 as colloidal using three types of liquid and two types of target by ablation in the liquid method. Thus, the impact of surfactant molecules on the optical, structural, and surface morphology properties of the prepared films from LN colloidal was examined for the first time.

2. Experimental Work

LiNbO_3 colloidal was prepared using ablation in liquid technique using a pulsed laser (PLAL). Two targets were employed: the first one is the LiNbO_3 Z-cut wafer sliced from LN bulk crystal; the second target was set by blending ultra-purity raw materials Lithium carbonate (Li_2CO_3), Niobium oxide (Nb_2O_5), and Ethanol ($\text{C}_2\text{H}_5\text{OH}$) which are processed in several steps to ensure that the pellet is ready to be used as a target for the ablation process, further information set out preparation steps reported in other studies [23]. LN target was placed in a glass vial in 5 and 2.5 mm^3 of liquid with LN pellet and LN Z-cut wafer respectively, it was illuminated by the second harmonic beam of a wavelength of (532 nm) of a Q-switched Nd: YAG laser operating at 1 Hz and 400 J/cm^2 laser fluence. Deionized water, acetone, and ethanol were consumed in the liquid environment. The laser beam was directed over onto the target with a diameter of approximately 1 mm. The optical absorption and transmission spectra were found using a UV–visible spectrometer (Perkin–Elmer, lambda 25). The optical energy gap of LiNbO_3 is evaluated using a graphical sketch via Tauc's equation for direct transitions as presented in Eq. (1) [24], [25]

$$(\alpha h\nu)^2 = A^2 (h\nu - E_g) \quad (1)$$

Where, α represent the absorption coefficient, E_g is the optical energy gap, $h\nu$ is the photon energy of the directed light while A is a constant. The correlation between both absorption coefficient (α) and extinction coefficient (K) is specified by the following relation (3) [26]:

$$K = \frac{\alpha \lambda}{4\pi} \quad (2)$$

To analyze structural qualities, an X-Ray Diffractometer (Panalytical X' Pert Pro) was employed. FESEM of (ZEISS SEGMA VP) was used to identify the morphology. Figure 1 a, and b show the PLAL setup, and a bulk schematic diagram showing step-by-step the preparation and characterization of the samples as mentioned elsewhere [27].

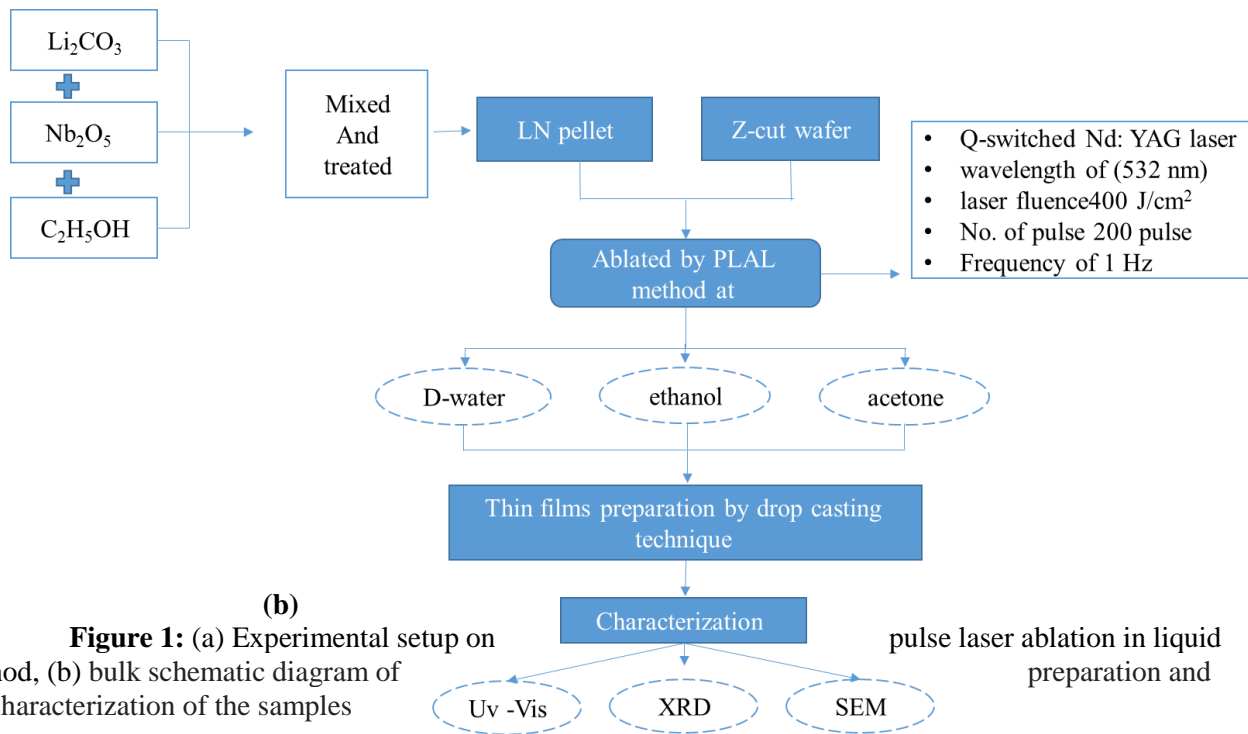
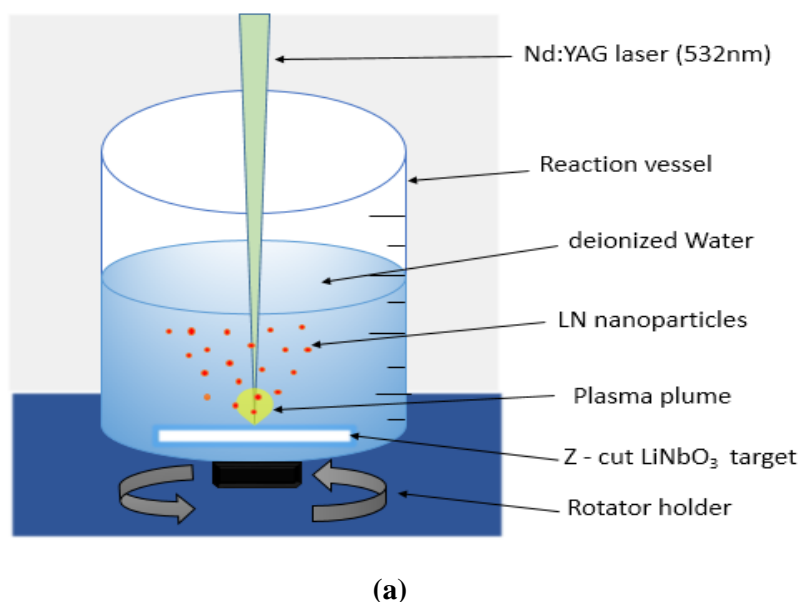


Figure 1: (a) Experimental setup on method, (b) bulk schematic diagram of characterization of the samples

pulse laser ablation in liquid preparation and

3. Results and Discussion

LiNbO₃ colloidal for the prepared LN target grow into brownish to yellow afterward the ablation procedure is completed, this may attribute to the fact different materials mix to get this target, dissolving one of the elements may cause this color, while samples prepared from the LN Z-cut wafer persist colorless and transparent after the ablation steps carried out. The transmission spectra for LiNbO₃ suspension prepared using the PLAL method in different liquids environments and for two types of targets are shown in Figure 2 a and b. In the case of pellet, the transmission spectra are about 88, 90, and 98% for ethanol, deionized water, and acetone respectively; however, for the Z-cut wafer of LN Transmission results showed a sharp edge with spectra of 96 and 98% for deionized water and ethanol respectively. Optical absorption of samples is in the UV range which is shown in Figure 3 a and b. for colloidal prepared using LN pellet deionized water and ethanol show two peaks small one at about 230 nm and another broad one at about 280 nm which almost match with the slight shift at the broader peak wing for the sample prepared in deionized water, while the acetone shows a small peak at 335 nm.

However, samples prepared from the LN wafer exhibit good features for ethanol with a peak at 264 nm and wide shoulder which may attribute to the quantum size effect which may indicate the formation of nanoparticles, while the deionized water sample shows a small peak at 218 nm and sharp shoulder. The blue shift of absorption peak result may explain by the meaning of the particle size change for different liquids having different dipole moments. This result came in good agreement with the energy gap value and FESM results.

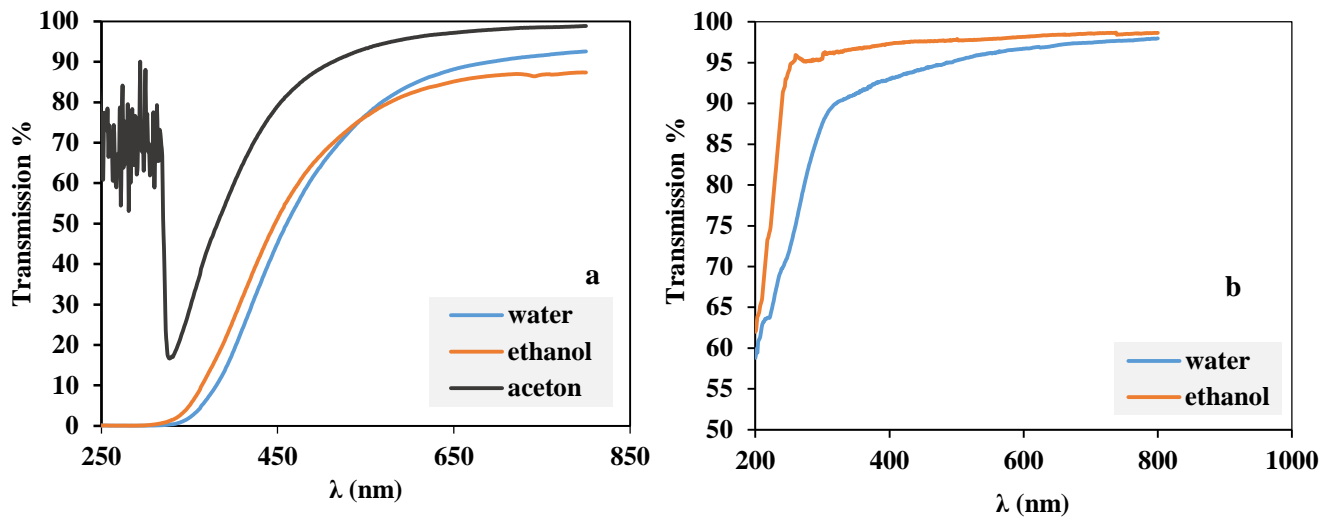


Figure 2: Transmission spectra of lithium-niobate suspension (a) LN pellet, (b) LN wafer.

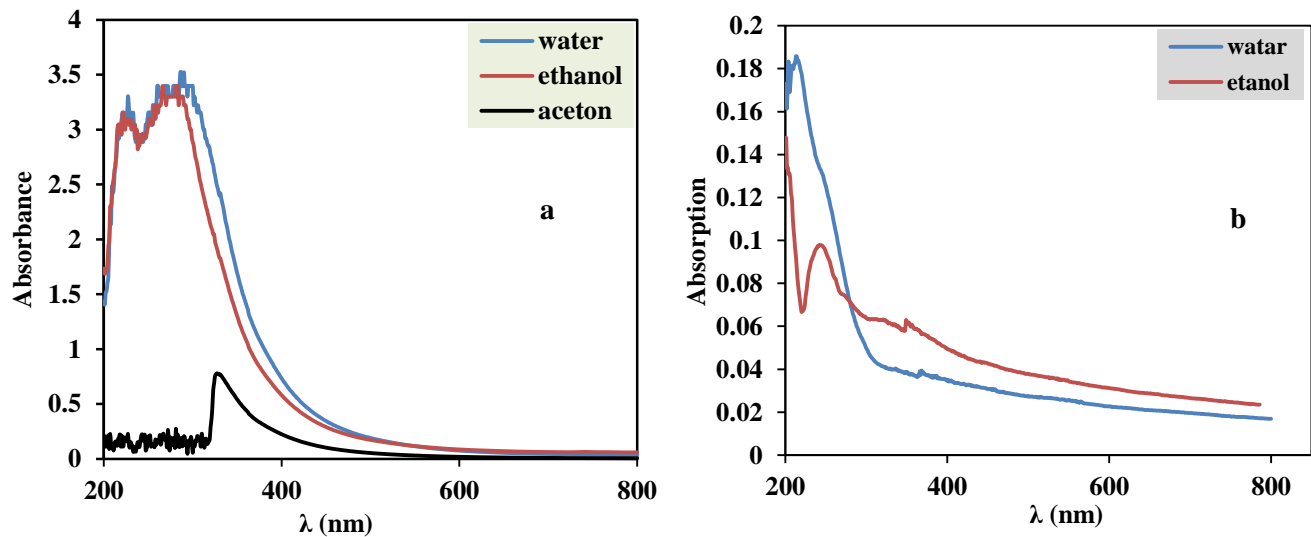


Figure 3: absorption spectra of lithium-niobate suspension (a) LN pellet, (b) LN wafer.

The significantly large optical energy gap inspires LiNbO_3 to be a good material for various probable applications, including the sensor, filters, and solar cells reducing window absorption losses, which may boost the short-circuit current (I_{sc}) of the used cells [23]. The energy gap value (E_g) is estimated by sketching $(\alpha h\nu)^2$ versus $h\nu$ as presented in Figure 4 a and b, the energy band gap value for samples prepared from LN Z-cut wafer is 4.3 eV for deionized water which is greater than ethanol samples of 4.1 eV indicating the variation in particles size of the prepared colloid, this may articulate by the fact that extremely polar molecules attract highly packed substantially stronger bounds towards the particle surface, therefore the repulsive electrostatic force due to overlapping of electrical double layers of both the nucleus and species in the plasma plume restrict further development, agglomeration and precipitation [19]. The dipole moment value of acetone liquid is about (2.88D), which is substantially higher than that of deionized water (1.85D), and later ethanol of about (1.69D). Growth by incorporating more species throughout the ablation process is depressed whenever the dipole moment is

significant, exactly like in deionized water, resulting in a lower particle size diameter beside a narrow distribution of size [19], [28]. The energy gap value for the LN prepared target shows a low energy gap value than the fundamental known value of 4 eV, which can be explained by the fact that this target is prepared by mixing lithium carbonate (Li_2CO_3), Niobium oxide (Nb_2O_5) and Ethanol liquid ($\text{C}_2\text{H}_5\text{OH}$), there always a chance of the unwanted reaction, of the undesirable element with liquid which may affect drastically the energy gap values.

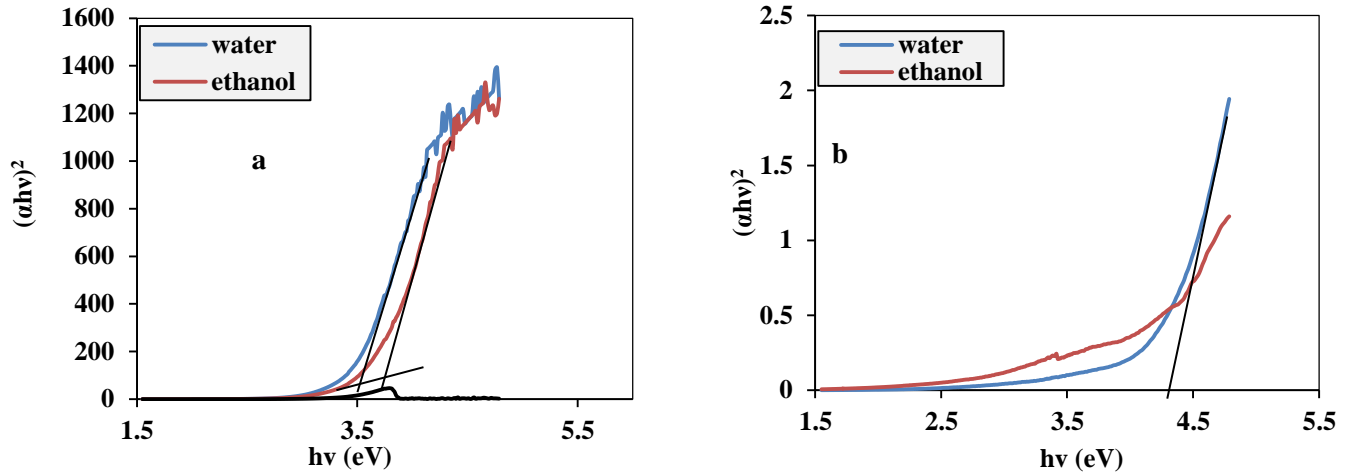


Figure 4: energy gap plots of $(\alpha hv)^2$ versus $h\nu$ of lithium-niobate suspension (a) LN pellet, (b) LN wafer.

The extinction coefficient (K) sketch as a function to $(h\nu)$ known as photon energy is displayed in Figure 5. The extinction coefficient is demonstrated to decrease with photon energy in the weak photon energy region up to certain photon energy. A good absorbing medium indicates a higher coefficient of extinction. The energy lost from electromagnetic radiation as it passes through a medium is defined by the material's coefficient K . Because the extinction coefficient is inversely proportional to the transmittance spectrum, a low transmittance leads to a high extinction coefficient, this may explain the very low value of K since all samples show high Transmission spectra value.

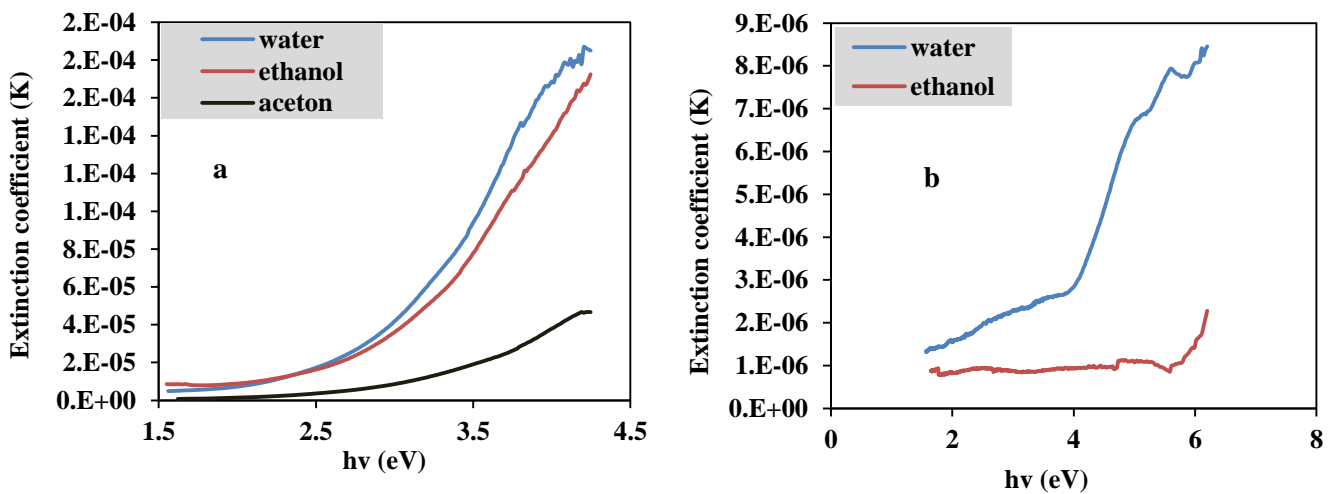


Figure 5: Extinction coefficient (K) of lithium-niobate suspension (a) LN pellet, (b) LN wafer.

Behavior of LiNbO_3 films is important. Epitaxial growth is preferable because, due to a refractive index mismatch at grain boundaries, it can decrease light dispersion. For certain applications, the growth behaviors with deposition parameters are more suitable to be managed instead of the substrate orientation or substrate type [29], [30]. Therefore, XDR analysis was carried out for both targets and wafers in water and ethanol. Figure 6 shows results for prepared samples prepared from target ablated in water with a mix of phases, desired ones like

(120), (400), (110), (600), and (024) plane at $2\theta = 24.72, 26.84, 35.52, 37.4, 47.44$ respectively, beside undesired secondary Li deficient phase LiNb_3O_8 at (602) planes and 2θ of 50.61, the presence of a secondary phase is evidence of the loss of lithium, which in turn leads to LiNb_3O_8 formation. Impurities of Nb_2O_5 were found at (101) corresponding to 37.4. Ethanol surrounding and target samples also show (120), (400), and (024) plane at $2\theta = 24.72, 26.84, \text{ and } 47.44$ respectively, beside impurities of Nb_2O_5 was at (101) related to 37.4, the presence of impurities may come from the ultra-purity raw materials (Li_2CO_3), (Nb_2O_5) and ($\text{C}_2\text{H}_5\text{OH}$), which are processed in several steps to have this target. These findings agree with optical results where a smaller energy gap is exhibited in these samples. The preferred phase for samples prepared from the compressed target is the (400) plane. While in Z-cut wafer there are no impurities like Nb_2O_5 , or secondary phase were detected, only peaks related to LN such as for water surrounding show a peak at 33.040, 47.70, 54.60, 56.40, 57.30, 61.70 belong to (104), (024), (116), (122), (018), (214) planes. Same peaks were observed for ethanol with wafer except for the 33.040 peaks. This indicated the formation of pure with multi orientation as shown in Figure 6 b. The XRD findings reveal that the Z-cut wafer demonstrates the best result with the domination of the (104) plane for samples prepared in the water and Z-cut wafer.

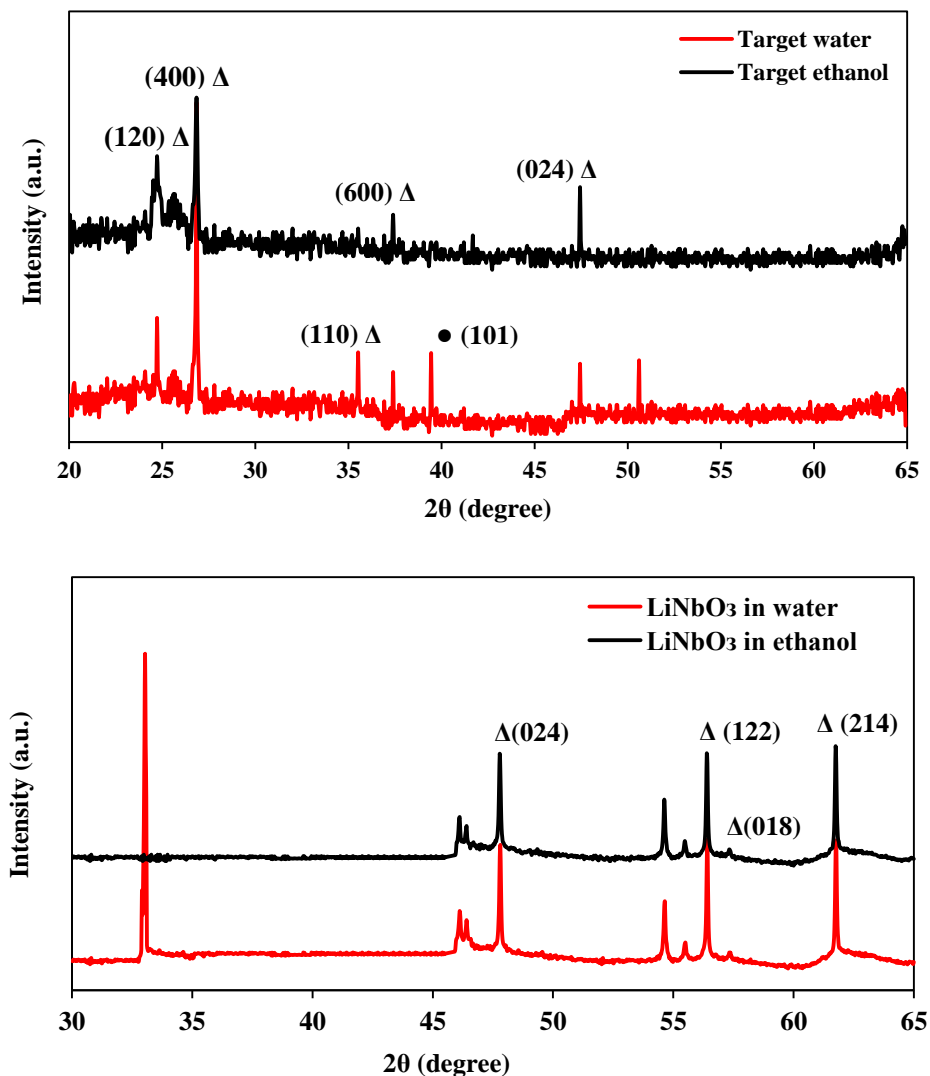


Figure 6: XRD of lithium-niobate thin films (a) LN pellet, (b) LN wafer.

Field Emission Scanning Electron Microscope (FESEM) of LiNbO_3 thin films were prepared in two different surfactants water and ethanol using a Z-cut wafer as a target to be ablated by the PLAL method. Samples were prepared at 1.3 J/cm^2 and 200 laser pulses as shown in Figure 7. The surface morphology of LN thin films shows

the particle size of ethanol is smaller than that of water by about 20 and 23 nm respectively. This result agrees with optical properties. The deposited films exhibit a spherical uniform and dense surface with merged particles' boundaries.

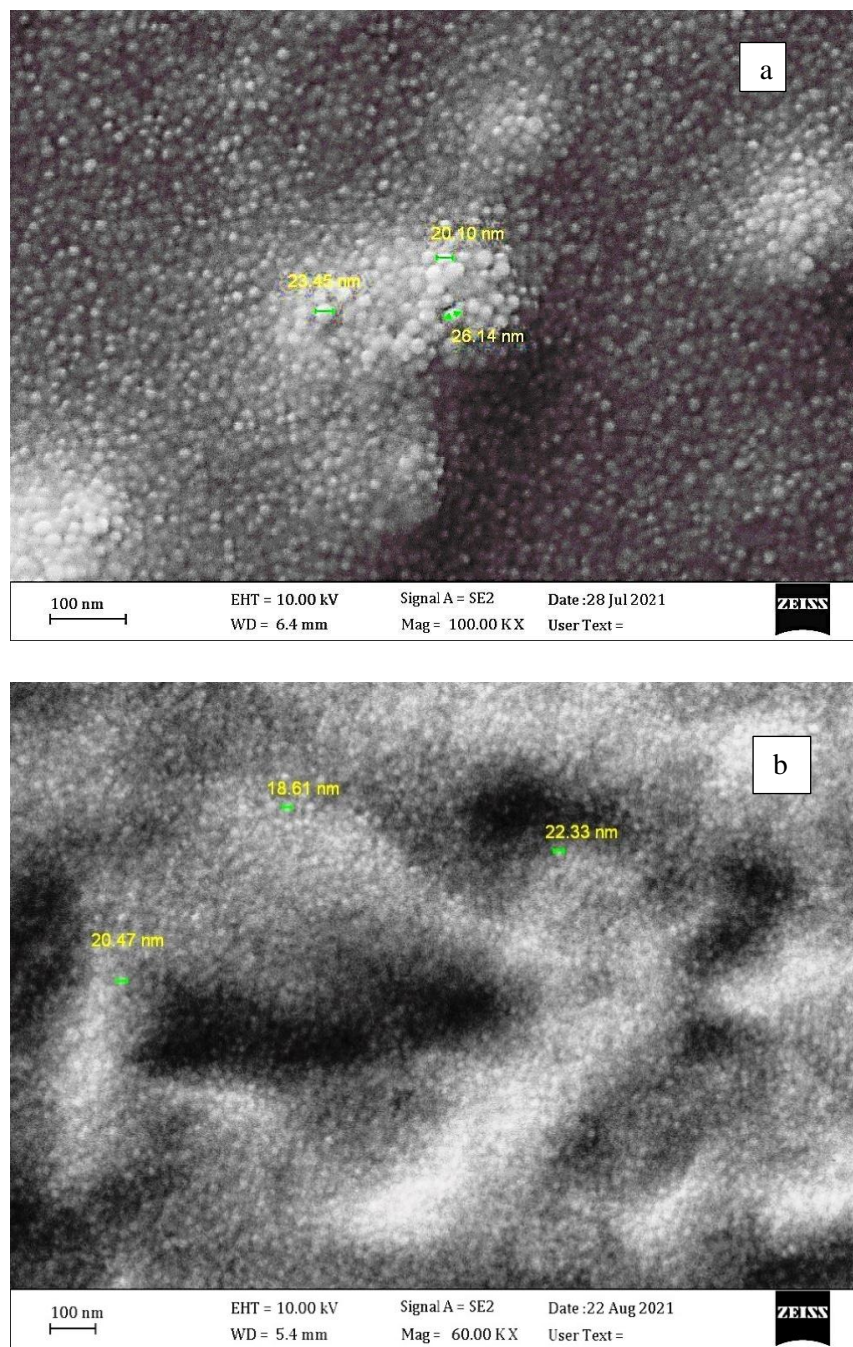


Figure 7: SEM image of LiNbO_3 prepared by PLAL using Z-cut wafer target (a) water, (b) ethanol liquid.

4. Conclusions

Pulsed laser ablation in the liquid route has been used successfully for the first time to prepare lithium niobate colloid nanoparticles using two types of target; the first one is a prepared target from a mix of ultra-purity raw materials and the second is cut in Z orientation from lithium niobate crystal. These two targets are used in three different liquids in the surrounding environment; deionized water, ethanol, and acetone. The absorption spectra and energy gap value of samples prepared from Z-cut LN wafer show promising starting results for LiNbO_3 suspension, which may be used further in many future applications, while a prepared target due to the presence

of impurities comes with undesirable results. The Acetone sample didn't show good quality results with the LN wafer, while ethanol and water exhibited better results with an energy gap near the known energy gap value for LN. XRD analysis shows that a prepared target is not desired if the pure preferred LN phase with no impurities is required for a certain application. However, the Z-cut crystal wafer is a good choice for this purpose with a multiphase of LiNbO_3 . FESEM results agree with the optical result concerning the formation of the nanosized spherical particles, especially for Z-cut wafer prepared in ethanol.

Acknowledgement

The authors would like to thank the department of laser engineering and electro-optic / University of Technology and phi center for the logistic support of this work.

Conflict of Interest

The authors have declared no conflict of interest.

References

- [1] R. S. Weis and T. K. Gaylord, "Lithium niobate: Summary of physical properties and crystal structure," *Appl. Phys. A Solids Surfaces*, vol. 37, no. 4, pp. 191–203, 1985.
- [2] M. S. A. A. Fakhri Makram, "preparation of nanophotonics LiNbO_3 thin films and studying their morphological and structural properties by sol -Gel method for waveguide application," *Int. J. Chem. Mol. Nucl. Mater. Metall. Eng.*, vol. 10, no. 5, pp. 435–440, 2016.
- [3] X. Yang *et al.*, "Cylindroid rigid-wall simulation of the influence of gas pressure in pulsed laser deposition of LiNbO_3 films," *Appl. Phys. Lett.*, vol. 82, no. 4, pp. 619–621, 2003.
- [4] F. Meriche *et al.*, "Fabrication and investigation of 1D and 2D structures in LiNbO_3 thin films by pulsed laser ablation," *Opt. Mater. (Amst.)*, vol. 32, no. 11, pp. 1427–1434, 2010.
- [5] X. Wang, Y. Liang, S. Tian, W. Man, and J. Jia, "Oxygen pressure dependent growth of pulsed laser deposited LiNbO_3 films on diamond for surface acoustic wave device application," *J. Cryst. Growth*, vol. 375, pp. 73–77, 2013.
- [6] M. Khatami, H. Q. Alijani, and I. Sharifi, "Biosynthesis of bimetallic and core-shell nanoparticles: Their biomedical applications - A review," *IET Nanobiotechnology*, vol. 12, no. 7, pp. 879–887, 2018.
- [7] W. C. Shih, T. L. Wang, X. Y. Sun, and M. S. Wu, "Growth of c-axis-oriented LiNbO_3 Films on $\text{ZnO/SiO}_2/\text{Si}$ substrate by pulsed laser deposition for surface acoustic wave applications," *Jpn. J. Appl. Phys.*, vol. 47, no. 5 PART 2, pp. 4056–4059, 2008.
- [8] C. E. Rüter, D. Brüske, S. Suntsov, and D. Kip, "Investigation of ytterbium incorporation in lithium niobate for active waveguide devices," *Appl. Sci.*, vol. 10, no. 6, 2020.
- [9] M. A. Fakhri *et al.*, "Physical investigations of nano and micro lithium-niobate deposited by spray pyrolysis technique," *AIP Conf. Proc.*, vol. 2045, 2018.
- [10] M. A. Fakhri *et al.*, "Enhancement of Lithium Niobate nanophotonic structures via spin-coating technique for optical waveguides application," *EPJ Web Conf.*, vol. 162, pp. 3–6, 2017.
- [11] R. S. Feigelson, "Epitaxial growth of lithium niobate thin films by the solid source MOCVD method," *J. Cryst. Growth*, vol. 166, no. 1–4, pp. 1–16, 1996.
- [12] E. S. P. B. V, "• L," vol. 99, pp. 630–633, 1990.
- [13] J. W. Son, S. S. Orlov, B. Phillips, and L. Hesselink, "Pulsed laser deposition of single phase LiNbO_3 thin film waveguides," *J. Electroceramics*, vol. 17, no. 2–4, pp. 591–595, 2006.
- [14] S. H. Lee and T. W. Noh, "Nonlinear optical properties of $\text{LiNbO}_3/\text{Al}_2\text{O}_3$ films epitaxially grown by pulsed laser deposition," *Integr. Ferroelectr.*, vol. 20, no. 1–4, pp. 25–37, 1998.
- [15] D. Hassan and M. Zayer, "Study and Investigation of the Effects of the OTA Technique on the Physical Properties of the ZnO Thin Films Prepared by PLD," *J. Appl. Sci. Nanotechnol.*, vol. 1, no. 4, pp. 32–43, 2021.
- [16] J. Gonzalo, C. N. Afonso, J. M. Ballesteros, A. Grosman, and C. Ortega, "Li deficiencies in LiNbO_3 films prepared by pulsed laser deposition in a buffer gas," *J. Appl. Phys.*, vol. 82, no. 6, pp. 3129–3133, 1997.
- [17] Z. Vakulov *et al.*, "Oxygen pressure influence on properties of nanocrystalline LiNbO_3 films grown by laser ablation," *Nanomaterials*, vol. 10, no. 7, pp. 1–13, 2020.
- [18] H. Zeng, W. Cai, Y. Li, J. Hu, and P. Liu, "Composition/structural evolution and optical properties of ZnO/Zn nanoparticles by laser ablation in liquid media," *J. Phys. Chem. B*, vol. 109, no. 39, pp. 18260–

18266, 2005.

- [19] G. Bajaj and R. K. Soni, "Effect of liquid medium on size and shape of nanoparticles prepared by pulsed laser ablation of tin," *Appl. Phys. A Mater. Sci. Process.*, vol. 97, no. 2, pp. 481–487, 2009.
- [20] S. S. Shaker, S. I. Younis, J. M. Moosa, and R. A. Ismail, "Pulsed laser deposition of nanostructured HgI₂ on Si substrate for photodetector application," *Mater. Sci. Semicond. Process.*, vol. 135, no. July, p. 106106, 2021.
- [21] I. Hasan, K. Khashan, and A. Hadi, "Study of the Effect of Laser Energy on the Structural and Optical Properties of TiO₂ NPs Prepared by PLAL Technique," *J. Appl. Sci. Nanotechnol.*, vol. 2, no. 1, pp. 11–19, 2022.
- [22] C. A. Perez-Lopez, J. A. Perez-Taborda, H. Riascos, and A. Avila, "The influence of pulsed laser ablation in liquids parameters on the synthesis of ZnO nanoparticles," *J. Phys. Conf. Ser.*, vol. 1541, no. 1, 2020.
- [23] S. M. Taleb, M. A. Fakhri, and S. A. Adnan, "Optical investigations of nanophotonic LiNbO₃ films deposited by pulsed laser deposition method," *Defect Diffus. Forum*, vol. 398 DDF, pp. 16–22, 2020.
- [24] T. M. Al-Saadi, B. H. Hussein, A. B. Hasan, and A. A. Shehab, "Study the structural and optical properties of Cr doped SnO₂ nanoparticles synthesized by sol-gel method," *Energy Procedia*, vol. 157, no. 2018, pp. 457–465, 2019.
- [25] A. J. Kadhm, R. A. Ismail, and A. F. Atwan, "Fabrication of Visible-Enhanced Nanostructured Mn₂O₃/Si Heterojunction Photodetector by Rapid Thermal Oxidation," *Silicon*, 2021.
- [26] R. A. Ismail, S. A. Zaidan, and R. M. Kadhim, "Preparation and characterization of aluminum oxide nanoparticles by laser ablation in liquid as passivating and anti-reflection coating for silicon photodiodes," *Appl. Nanosci.*, vol. 7, no. 7, pp. 477–487, 2017.
- [27] R. A. Ismail, S. Erten-Ela, A. K. Ali, C. Yavuz, and K. I. Hassoon, "Pulsed Laser Ablation of Tin Oxide Nanoparticles in Liquid for Optoelectronic Devices," *Silicon*, vol. 13, no. 9, pp. 3229–3237, 2021.
- [28] J. M. Moosa, R. A. Ismail, and J. H. Khulaife, "Structural, Optical and Electrical Properties of KCsI₂ Film Deposited by Spray Pyrolysis," *J. Phys. Conf. Ser.*, vol. 1795, no. 1, 2021.
- [29] S. H. Lee, T. W. Noh, and J. H. Lee, "Control of epitaxial growth of pulsed laser deposited LiNbO₃ films and their electro-optic effects," *Appl. Phys. Lett.*, vol. 472, p. 472, 1995.
- [30] E. T. Salim, Y. Al-Douri, M. S. Al Wazny, and M. A. Fakhri, "Optical properties of Cauliflower-like Bi nanostructures by reactive pulsed laser deposition (PLD) technique," *Sol. Energy*, vol. 107, 2014.